

Article

# Schwarzschild Black Holes in Extended Spacetime with Two Time Dimensions

Mechid Paiman <sup>1,\*</sup>, Horia Cornean <sup>2</sup> and Christoph Köhn <sup>1,\*</sup> <sup>1</sup> National Space Institute (DTU Space), Technical University of Denmark, DK-2800 Kongens Lyngby, Denmark<sup>2</sup> Department of Mathematical Sciences, Aalborg University, DK-9220 Aalborg Øst, Denmark; cornean@math.aau.dk

\* Correspondence: s194730@student.dtu.dk (M.P.); koehn@space.dtu.dk (C.K.)

**Abstract:** Black holes are one of the most extreme phenomena in the Universe, bridging the gap between the realms of general relativity and quantum physics. Any matter that crosses the event horizon moves towards the core of the black hole, creating a singularity with infinite mass density—a phenomenon that cannot be comprehended within present theories of relativity and quantum physics. In this study, we undertake an investigation of non-rotating, non-charged Schwarzschild black holes in an extended spacetime framework with two time dimensions. To accomplish this, we extend Einstein’s field equations by one more temporal dimension. We solve the corresponding equations for a spherical central mass, which leads to an Abel-type equation for the 5D Schwarzschild metric. By exploring distinct solution classes, we present an approximate solution for the 5D metric. Our proposed solution maintains consistency with Schwarzschild’s 4D solution. Finally, we address the central black hole singularity and demonstrate a potential breakthrough, as our solution effectively avoids the singularity quandary, providing valuable insight into the fundamental properties of black holes in this augmented framework.

**Keywords:** Schwarzschild black holes; extended spacetime; two time dimensions; black hole singularity



**Citation:** Paiman, M.; Cornean, H.; Köhn, C. Schwarzschild Black Holes in Extended Spacetime with Two Time Dimensions. *Astronomy* **2023**, *2*, 269–285. <https://doi.org/10.3390/astronomy2040018>

Academic Editor: Pedro Bargueno

Received: 11 September 2023

Revised: 24 October 2023

Accepted: 30 October 2023

Published: 6 November 2023



**Copyright:** © 2023 by the authors. Licensee MDPI, Basel, Switzerland. This article is an open access article distributed under the terms and conditions of the Creative Commons Attribution (CC BY) license (<https://creativecommons.org/licenses/by/4.0/>).

## 1. Introduction

Black holes are one of the most extreme phenomena in our Universe. They are spherical bodies consisting of masses ranging from tens to millions of solar masses [1] and are purely characterized by their mass, angular momentum, and charge, which is also known as the “No-Hair theorem” [2]. After Einstein had finalized the concept of general relativity in 1915 [3], Schwarzschild calculated its first exact solution [4] which describes spacetime around spherical, non-rotating, non-charged massive bodies, including black holes. Building upon Schwarzschild’s work, other notable solutions have emerged for black holes that are rotating or are electrically charged [5–10]. Roger Penrose showed that black holes are common objects in our Universe [11], and recent observational efforts by the Event Horizon Telescope have provided visual evidence of black holes, such as M87\* in the galaxy Messier 87 [12] and Sagittarius A\* in our own Milky Way [13].

The intense gravitational pull of black holes curves spacetime to such an extent that any particle in their vicinity is drawn towards their interior, which is separated from its exterior by the event horizon. Every particle, including photons, passing through the event horizon inevitably moves to the black hole center, where all the mass accumulates in a single point, generating an infinitely large mass density—a singularity. The interior of black holes poses challenges from both observational and theoretical viewpoints. Due to the event horizon’s nature, no information can escape from the inside, making it currently impossible to observationally gain information about the inner workings of black holes. From a theoretical perspective, the laws of general relativity collapse at the center because of the singularity, calling for a future theory of quantum gravity [14] which would unify the principles of relativity with subatomic quantum principles.

Promising candidates for quantum gravity are loop quantum gravity [15] and string theory [16]. Following Hawking's recent proposal that gravitational collapse may not produce event horizons, Vaz introduces a unique perspective on black holes without event horizons. He instead suggests they are quantum objects with matter condensing on the apparent horizon during a quantum collapse [17]. Corda expanded on this concept, showing that these black holes possess an atomic structure governed by quantum mechanics and deriving mass and energy using a Schrödinger-like approach [18]. String theory, on the other hand, suggests the existence of 10 or 26 spatial dimensions, which is significantly more than the commonly experienced three space dimensions. These extra dimensions are assumed to be compactified and are consequently too small to be observed. In exploring the concept of extra dimensions, Bars et al. demonstrated that a certain class of string theories could also obtain more than one time dimension [19]. This idea was further developed by Bars and Kounnas when they constructed actions for interacting p-branes within two time dimensions and presented a Kaluza–Klein-like dimensional reduction mechanism, along with an action for a string in two time dimensions [20,21]. However, one of the difficulties with such theories is that extra macroscopic temporal dimensions might violate causality or cause to an unstable or unpredictable universe [22], especially for three spatial dimensions. Therefore, any extra time dimension must be microscopic or act on spatial scales in the order of the Planck length [23].

The idea of additional time dimensions was taken over by Chen who interpreted two extra time dimensions as hidden quantum variables. He demonstrated that the concept of matter waves, using the de Broglie wavelength, naturally arises from the action of a free particle in several time dimensions [24]. Köhn later proposed that the existence of a second time dimension could explain the constancy of the speed of light and provide a theoretical foundation for the existence of a minimum length scale known as the Planck length [23]. When extending the Einstein–Friedmann equations for the evolution of the Universe, Köhn could constrain the value of the cosmological constant and provide a possible solution to the cosmological constant problem [25]. More recently, a two-time-dimensional version of Maxwell's equations has allowed symmetrizing them and introducing magnetic monopoles. This framework also provides a plausible explanation for why magnetic monopoles have not been observed, suggesting that they are hidden in the second non-observable time dimension [26]. While physical arguments have not necessarily favored theories with more than one time dimension, Weinstein and Craig [27,28] arrived at well-posed solutions for equations such as the five-dimensional wave equation, indicating the feasibility of known mathematics in a universe with two time dimensions and hence of its physical reality.

In this study, we aim to investigate the modifications in the properties of Schwarzschild black holes when considering an extended spacetime with three spatial and two temporal dimensions. Our primary focus is on understanding how the Schwarzschild metric changes within its extended spacetime framework and exploring different classes of solutions. Ultimately, we seek to evaluate the nature of singularity at the centers of black holes in this extended spacetime.

In Section 2, we present the derivation of the 5D Schwarzschild equations. Section 3 explores solutions for these 5D equations. Firstly, we examine the existence of such solutions in both 4D and 5D contexts. Subsequently, we investigate various solution classes. Finally, in Section 4, we provide a physical interpretation of our findings, considering the limits in which the 5D framework behaves like the familiar 4D scenario. This contributes to resolving the singularity problem.

### 2. 5D Schwarzschild Equations

In this section, we derive the Einstein field equations for the five-dimensional Schwarzschild metric. The starting point is to extend the four-vector of spacetime to a five-vector:

$$\vec{x}^\mu = \begin{pmatrix} x^0 \\ x^1 \\ x^2 \\ x^3 \\ x^4 \end{pmatrix} = \begin{pmatrix} ct \\ \gamma\tau \\ r \\ \theta(r) \\ \varphi(r) \end{pmatrix} \tag{1}$$

where  $\gamma$  represents a characteristic velocity for the second time, equivalent to the speed of light  $c$  for the first time  $t$ . Similarly, we extend the four-dimensional ansatz for the metric of spacetime in the vicinity of a spherical body to five dimensions,

$$g_{\mu\nu} = \begin{pmatrix} A(r) & 0 & 0 & 0 & 0 \\ 0 & Z(r) & 0 & 0 & 0 \\ 0 & 0 & -B(r) & 0 & 0 \\ 0 & 0 & 0 & -r^2 & 0 \\ 0 & 0 & 0 & 0 & -r^2 \sin^2(\theta) \end{pmatrix} \tag{2}$$

where  $A(r)$  and  $B(r)$  correspond to the first, macroscopic time dimension and  $Z(r)$  describes the contribution of the second time dimension.

For this ansatz (2), there exist 16 nonzero Christoffel symbols,

$$\begin{aligned} \Gamma_{02}^0 &= \Gamma_{20}^0 = \frac{A'}{2A} \\ \Gamma_{12}^1 &= \Gamma_{21}^1 = \frac{Z'}{2Z} \\ \Gamma_{00}^2 &= \frac{A'}{2B} \\ \Gamma_{11}^2 &= \frac{Z'}{2B} \\ \Gamma_{22}^2 &= \frac{B'}{2B} \\ \Gamma_{33}^2 &= -\frac{r}{B} \\ \Gamma_{44}^2 &= -\frac{r \sin^2(\theta)}{B} \\ \Gamma_{23}^3 &= \Gamma_{32}^3 = \Gamma_{24}^4 = \Gamma_{42}^4 = \frac{1}{r} \\ \Gamma_{44}^3 &= -\cos(\theta) \sin(\theta) \\ \Gamma_{34}^4 &= \Gamma_{43}^4 = \cot(\theta) \end{aligned} \tag{3}$$

where the prime denotes the derivative with respect to  $r$ . These lead to the following Ricci tensor components

$$R_{00} = \frac{A''}{2B} - \frac{A'B'}{4B^2} + \frac{A'}{Br} - \frac{(A')^2}{4AB} + \frac{A'Z'}{4ZB} \tag{4}$$

$$R_{11} = \frac{Z''}{2B} - \frac{Z'B'}{4B^2} + \frac{Z'}{Br} - \frac{(Z')^2}{4ZB} + \frac{A'Z'}{4AB} \tag{5}$$

$$R_{22} = -\frac{A''}{2A} + \frac{(A')^2}{4A^2} + \frac{A'B'}{4AB} + \frac{B'}{Br} - \frac{Z''}{2Z} + \frac{(Z')^2}{4Z^2} + \frac{Z'B'}{4ZB} \tag{6}$$

$$R_{33} = -\frac{1}{B} + 1 - \frac{rA'}{2AB} + \frac{rB'}{2B^2} - \frac{rZ'}{2ZB} \tag{7}$$

$$R_{44} = R_{33} \sin^2(\theta). \tag{8}$$

The Ricci scalar then becomes

$$R = \frac{10}{3} \Lambda. \tag{9}$$

For the Schwarzschild solution, we consider a vacuum around the central mass,  $T_{\mu\nu} = 0$ . Hence, the 5D Einstein equations

$$R_{\mu\nu} - \frac{1}{2}Rg_{\mu\nu} + \Lambda g_{\mu\nu} = 0 \tag{10}$$

For the ansatz (2), together with (4)–(9), lead to a set of four equations:

$$2ABrA'' - ArA'B' - Br(A')^2 + \frac{ABrA'Z'}{Z} + 4ABA' - \frac{8}{3}A^2B^2r\Lambda = 0 \tag{11}$$

$$2ZBrZ'' - ZrZ'B' - Br(Z')^2 + \frac{ZBrA'Z'}{A} + 4ZBZ' - \frac{8}{3}Z^2B^2r\Lambda = 0 \tag{12}$$

$$-2ABrA'' + ArA'B' + Br(A')^2 - \frac{2A^2BrZ''}{Z} + \frac{A^2Br(Z')^2}{Z^2} + \frac{A^2rB'Z'}{Z} + 4A^2B' + \frac{8}{3}A^2B^2r\Lambda = 0 \tag{13}$$

$$-2AB + ArB' - BrA' - \frac{ABrZ'}{Z} + 2AB^2 + \frac{4}{3}AB^2r^2\Lambda = 0. \tag{14}$$

Equations (11)–(14) are equivalent to the field equations in 4D but with additional terms involving  $Z$  associated with the second time dimension. Equation (12) is an additional equation purely based on the second time dimension and is identical to Equation (11) except with  $Z$  substituting  $A$ . The set of Equations (11)–(14) can be reduced to first order by defining  $a = \frac{A'}{A}$ ,  $z = \frac{Z'}{Z}$ , and  $b = \frac{B'}{B}$ :

$$2ra' + ra^2 - rab + raz + 4a - \frac{8}{3}Br\Lambda = 0 \tag{15}$$

$$2rz' + rz^2 - rzb + raz + 4z - \frac{8}{3}Br\Lambda = 0 \tag{16}$$

$$-2ra' - 2rz' - ra^2 - rz^2 + rab + rzb + 4b + \frac{8}{3}Br\Lambda = 0 \tag{17}$$

$$-2 - ra - rz + rb + 2B + \frac{4}{3}Br^2\Lambda = 0. \tag{18}$$

This set is reduced to the 4D field equations for the Schwarzschild metric when  $z = 0$ . Additionally, the system (15)–(18) is overdetermined as it contains four equations for the three functions  $A$ ,  $Z$ , and  $B$ , which define  $a$ ,  $z$ , and  $b$ . Note that these equations explicitly still contain  $B$ , which defines  $b$ . We will discuss this in the next section.

### 3. Solution of 5D Equations

As mentioned previously, the system (15)–(18) is overdetermined. Therefore, we first demonstrate the existence of a solution. Subsequently, we derive and discuss several classes of solutions before presenting an approximate solution to Equations (15)–(18). As we show below, the system can be reduced to an Abel equation, which cannot be solved analytically.

#### 3.1. Existence of a Solution

To show the existence of a solution, we begin by adding Equations (15)–(17), yielding:

$$2b - \frac{4}{3}r\Lambda B = -2a - 2z - raz. \tag{19}$$

Together with Equation (18), this generates an algebraic system of two linear equations for the unknowns  $b$  and  $B$ . The solution, depending on  $a$  and  $z$ , is given by

$$B = \frac{1 + ra + rz + \frac{r^2 az}{4}}{1 + r^2 \Lambda}, \quad (20)$$

$$b = \frac{\frac{2}{3} r \Lambda B - a - z - \frac{raz}{2}}{\frac{2}{3} r \Lambda - \frac{1}{3} r^3 az \Lambda - a - z - \frac{raz}{2} - \frac{1}{3} r^2 \Lambda (a + z)} = \frac{\frac{2}{3} r \Lambda B - a - z - \frac{raz}{2}}{1 + r^2 \Lambda}. \quad (21)$$

Furthermore, (18) can be written as

$$rb = 2 + ra + rz - \left(2 + \frac{4}{3} r^2 \Lambda\right) B. \quad (22)$$

Multiplying (22) by  $a$ ,

$$rab = 2a + ra^2 + raz - \left(2 + \frac{4}{3} r^2 \Lambda\right) aB, \quad (23)$$

And inserting it into (15), we obtain

$$2ra' + 2a + \left(2a + \frac{4}{3} r^2 a \Lambda - \frac{8}{3} r \Lambda\right) B = 0. \quad (24)$$

Similarly, multiplying (22) by  $z$  and introducing it into (16), we obtain

$$2rz' + 2z + \left(2z + \frac{4}{3} r^2 z \Lambda - \frac{8}{3} r \Lambda\right) B = 0. \quad (25)$$

By introducing Equation (20) into Equations (24) and (25), we obtain a self-contained system of two first-order nonlinear differential equations involving  $a$  and  $z$ :

$$\frac{a + ra'}{1 + ra + rz + \frac{r^2 az}{4}} = \frac{-a - \frac{2}{3} r^2 a \Lambda + \frac{4}{3} r \Lambda}{1 + r^2 \Lambda} \quad (26)$$

$$\frac{z + rz'}{1 + ra + rz + \frac{r^2 az}{4}} = \frac{-z - \frac{2}{3} r^2 z \Lambda + \frac{4}{3} r \Lambda}{1 + r^2 \Lambda}. \quad (27)$$

This reduced system obeys the conditions of the local existence and uniqueness theorem [29], and thus provides a solution to the full system (15)–(18) if we can also show that  $b = \frac{B'}{B}$  is automatically satisfied. By differentiating (20), we obtain

$$B' = \frac{\left(a + z + ra' + rz' + \frac{raz}{2} + \frac{r^2 a' z}{4} + \frac{r^2 az'}{4}\right)}{(1 + r^2 \Lambda)} - \frac{\left(1 + ra + rz + \frac{r^2 az}{4}\right) 2r \Lambda}{(1 + r^2 \Lambda)^2}. \quad (28)$$

To force the appearance of the factor  $B$  on the right-hand side, we rewrite (28) as

$$B' = B \left( \frac{a + z + ra' + rz' + \frac{raz}{2} + \frac{r^2 a' z}{4} + \frac{r^2 az'}{4}}{1 + ra + rz + \frac{r^2 az}{4}} - \frac{2r \Lambda}{1 + r^2 \Lambda} \right). \quad (29)$$

We observe the identity

$$a + z + ra' + rz' + \frac{raz}{2} + \frac{r^2 a' z}{4} + \frac{r^2 az'}{4} = (a + ra') \left(1 + \frac{rz}{4}\right) + (z + rz') \left(1 + \frac{ra}{4}\right) \quad (30)$$

which, coupled with the system (26)–(27), leads to

$$B' = B \left( \frac{\left(-a - \frac{2}{3}r^2a\Lambda + \frac{4}{3}r\Lambda\right)\left(1 + \frac{rz}{4}\right) + \left(-z - \frac{2}{3}r^2z\Lambda + \frac{4}{3}r\Lambda\right)\left(1 + \frac{ra}{4}\right) - 2r\Lambda}{1 + r^2\Lambda} \right). \tag{31}$$

Comparing (31) with (21), we observe that the fraction on the right-hand side indeed equals  $b$ , and thus  $b = \frac{B'}{B}$  is satisfied. This concludes the proof of the existence of a solution to the 5D equations. As the 4D case results from (15)–(18) for  $z = 0$ , this also proves the existence of a solution for four spacetime dimensions.

### 3.2. Solution Classes

In this section, we will derive an Abel equation for the variable  $a$ . It is important to note that the cosmological constant  $\Lambda \cong 10^{-52} \text{ m}^2$  has a negligible contribution to the final solution of the metric around and inside the event horizon. Therefore, we set it to 0. The resulting system of Equations (15)–(18) becomes

$$2ra' + ra^2 - rab + raz + 4a = 0 \tag{32}$$

$$2rz' + rz^2 - rzb + raz + 4z = 0 \tag{33}$$

$$-2ra' - 2rz' - ra^2 - rz^2 + rab + rzb + 4b = 0 \tag{34}$$

$$-2 - ra - rz + rb + 2B = 0. \tag{35}$$

By isolating  $b$  in (32), we obtain

$$b = \frac{4a + ra^2 + raz + 2ra'}{ra} \tag{36}$$

which we insert into (33), resulting in

$$z = aC_1. \tag{37}$$

Here, without the loss of generality, we assume  $C_1 > 0$ . Therefore, knowing a solution for  $a$  (thus  $A$ ) allows us to calculate solutions for  $b$  and  $z$ , and thus finally for  $B$  and  $Z$ .

When substituting expression (37) for  $z$  into the system (32)–(35), Equation (32) equals (33), simplifying the system with the resulting equations:

$$2ra' + ra^2 - rab + ra^2C_1 + 4a = 0 \tag{38}$$

$$-2ra' - 2ra'C_1 - ra^2 - ra^2C_1^2 + rab + rabC_1 + 4b = 0 \tag{39}$$

$$-2 - ra - raC_1 + rb + 2B = 0. \tag{40}$$

By inserting (36) into (38), we obtain an Abel equation for  $a$ :

$$a + ra' + a \left( 1 + raC_1 + ra + \frac{r^2a^2C_1}{4} \right) = 0. \tag{41}$$

It is worth noting that when  $C_1 = 0$ , this equation is reduced to

$$2a + ra' + ra^2 = 0 \tag{42}$$

and

$$b = \frac{2ra' + ra^2 + 4a}{ra} \tag{43}$$

which, together with (36), are the corresponding equations for the 4D Schwarzschild metric with  $z = 0$ .

Hence, neglecting the influence of the second time dimension. The 4D Equations (42) and (43) yield the exact solutions

$$a_{4D} = \frac{1}{r\left(\frac{r}{r_S} - 1\right)} \tag{44}$$

$$b_{4D} = -\frac{r_S}{r(r - r_S)} \tag{45}$$

where the Schwarzschild radius  $r_S = \frac{2GM}{c^2}$  is related to the mass of the central object [4]. The corresponding solutions for  $A$  and  $B$  are

$$A_{4D} = 1 - \frac{r_S}{r} \tag{46}$$

$$B_{4D} = \frac{r}{r - r_S} = \left(1 - \frac{r_S}{r}\right)^{-1}. \tag{47}$$

Let us now continue analyzing Equation (41).

Using the definitions

$$\alpha_{>} = \frac{-(1 + C_1) + \sqrt{1 + C_1 + C_1^2}}{\frac{C_1}{2}} \tag{48}$$

$$\alpha_{<} = \frac{-(1 + C_1) - \sqrt{1 + C_1 + C_1^2}}{\frac{C_1}{2}} \tag{49}$$

The Abel Equation (41) can be rewritten as

$$(ra)' = -a\left(\frac{C_1}{4}\right)(ra - \alpha_{<})(ra - \alpha_{>}) \tag{50}$$

with the implicit solution

$$\ln|ra| + \frac{\alpha_{<}\ln|ra - \alpha_{>}| - \alpha_{>}\ln|ra - \alpha_{<}|}{\alpha_{>} - \alpha_{<}} = \ln\left(\frac{r_{S,5D}}{r}\right), \tag{51}$$

using  $r_{S,5D}$  as the integration constant. Note that both  $\alpha_{>}$  and  $\alpha_{<}$  are negative for  $C_1 > 0$ . For  $C_1 \rightarrow 0$ , the asymptotic behaviors are as follows:

$$\alpha_{>} \sim -1 \tag{52}$$

$$C_1\alpha_{>} \sim -C_1 \tag{53}$$

$$C_1\alpha_{>}^2 \sim -4C_1^2 \tag{54}$$

$$\alpha_{<} \sim -\frac{4}{C_1} \tag{55}$$

$$C_1\alpha_{<} \sim -4 \tag{56}$$

$$C_1 \alpha_{<}^2 \sim \frac{16}{C_1}. \tag{57}$$

Similarly, the asymptotic behaviors for  $C_1 \rightarrow \infty$  are

$$\alpha_{>} \sim -\frac{1}{C_1} \tag{58}$$

$$C_1 \alpha_{>} \sim -1 \tag{59}$$

$$C_1 \alpha_{>}^2 \sim \frac{1}{C_1} \tag{60}$$

$$\alpha_{<} \sim -4 \tag{61}$$

$$C_1 \alpha_{<} \sim -4C_1 \tag{62}$$

$$C_1 \alpha_{<}^2 \sim 16C_1. \tag{63}$$

Based on the initial condition  $a(r_0)$ , we can classify the solutions into different classes. The first three cases cover situations where  $r_0 a(r_0) < 0 \leftrightarrow a(r_0) < 0$ , which, due to the 4D solution (44), we can interpret as being inside the event horizon. Case (iv) with  $r_0 a(r_0) > 0$  is supposed to be outside of the event horizon. An overview is found in Table 1:

**Table 1.** Overview of solution classes.

Solution Classes	
(i)	$\alpha_{<} < r_0 a(r_0) < \alpha_{>} < 0$
(ii)	$\alpha_{<} < \alpha_{>} < r_0 a(r_0) < 0$
(iii)	$r_0 a(r_0) < \alpha_{<} < \alpha_{>} < 0$
(iv)	$0 < r_0 a(r_0)$

For these different cases, we explore the asymptotic behavior of the solutions for  $r \rightarrow 0$ ,  $r \rightarrow \infty$ , and  $r \rightarrow r_{S,5D}$  where needed. Note that for a complete description of the metric in the limit  $r \rightarrow \infty$ , the cosmological constant would be needed. However, since we only use the limits to check the consistency with the 4D Schwarzschild solutions (46) and (47) for  $C_1 \rightarrow 0$  without cosmological constant [4], and since we focus on the environment and interior of black holes, we refrain from including the cosmological constant in our solutions.

(i)  $\alpha_{<} < r_0 a(r_0) < \alpha_{>} < 0$ : In this case, it follows from (50) that  $(ra)' < 0$  for all  $r > 0$ .

Taking the limit  $r \rightarrow 0$  in (51),  $ra$  converges to  $\alpha_{>}$  as  $\frac{\alpha_{<}}{\alpha_{>} - \alpha_{<}} < 0$  and thus  $a$  behaves like  $a \sim \frac{\alpha_{>}}{r}$ , such that

$$A \sim r^{\alpha_{>}}. \tag{64}$$

Similarly,  $z \sim C_1 \alpha_{>} r$ , leading to

$$Z \sim r^{C_1 \alpha_{>}}. \tag{65}$$

Then, with the help of (53),

$$B \sim 1 + \alpha_{>} + C_1 \alpha_{>} + \frac{1}{4} C_1 \alpha_{>}^2. \tag{66}$$

We now consider the limits  $C_1 \rightarrow 0$  and  $C_1 \rightarrow \infty$ , which yield the following asymptotic behaviors:

$$A \sim r^{-1} \tag{67}$$

$$Z \sim r^{-C_1} \tag{68}$$

$$B \sim -C_1 - C_1^2 \tag{69}$$

for  $C_1 \rightarrow 0$  and

$$A \sim r^{-\frac{1}{C_1}} \tag{70}$$

$$Z \sim r^{-1} \tag{71}$$

$$B \sim -\frac{3}{4C_1} \tag{72}$$

for  $C_1 \rightarrow \infty$ .

Moreover, if  $r \rightarrow \infty$ , then  $ra \rightarrow \alpha_<$ . Subsequently,  $a \sim \frac{\alpha_<}{r}$ , and using the same analysis as for  $r \rightarrow 0$ , we find:

$$A \sim r^{\alpha_<} \tag{73}$$

$$Z \sim r^{C_1 \alpha_<} \tag{74}$$

$$B \sim 1 + \alpha_< + C_1 \alpha_< + \frac{1}{4} C_1 \alpha_<^2. \tag{75}$$

The asymptotic behaviors of (73)–(75) are

$$A \sim r^{-\frac{4}{C_1}} \tag{76}$$

$$Z \sim r^{-4} \tag{77}$$

$$B \sim -3 \tag{78}$$

for  $C_1 \rightarrow 0$  and

$$A \sim r^{-4} \tag{79}$$

$$Z \sim r^{-4C_1} \tag{80}$$

$$B \sim -3 \tag{81}$$

for  $C_1 \rightarrow \infty$ .

The results for  $A$ ,  $Z$ , and  $B$  are summarized in Table 2. Note that for  $C_1 \rightarrow 0$ , which represents the limit of a vanishing second time dimension, the solutions for  $A$  and  $B$  exhibit the same asymptotic behavior as  $A_{4D}$  (46) and  $B_{4D}$  (47), thus remaining consistent with the 4D solution.

**Table 2.** Asymptotic solution for case (i),  $\alpha_{<} < r_0a(r_0) < \alpha_{>} < 0$  for  $r \rightarrow 0, \infty$  and  $C_1 \rightarrow 0, \infty$ .

		$r \rightarrow 0$	$r \rightarrow \infty$
A	$C_1 \rightarrow 0$	$r^{-1}$	$r^{-\frac{4}{C_1}}$
	$C_1 \rightarrow \infty$	$r^{-\frac{1}{C_1}}$	$r^{-4}$
Z	$C_1 \rightarrow 0$	$r^{-C_1}$	$r^{-4}$
	$C_1 \rightarrow \infty$	$r^{-1}$	$r^{-4C_1}$
B	$C_1 \rightarrow 0$	$-C_1 - C_1^2$	$-3$
	$C_1 \rightarrow \infty$	$-\frac{3}{4C_1}$	$-3$

(ii)  $\alpha_{<} < \alpha_{>} < r_0a(r_0) < 0$ : In this case,  $(ra)' > 0$ .

In the limit  $r \rightarrow 0$ ,  $a$  behaves similarly to case (i), with  $a \sim \frac{\alpha_{>}}{r}$ . As  $r$  approaches infinity,  $a$  behaves as  $a \sim -\frac{1}{r^2}$ , which implies the following asymptotic solutions:

$$A \sim e^{\frac{1}{r}} \tag{82}$$

$$Z \sim e^{\frac{C_1}{r}} \tag{83}$$

$$B \sim 1 - \frac{1}{r} - \frac{C_1}{r} + \frac{C_1}{4r^2}. \tag{84}$$

Performing a similar analysis as for case (i), we can determine the asymptotic behavior for  $C_1 \rightarrow 0$  and  $C_1 \rightarrow \infty$ , as summarized in Table 3.

**Table 3.** Asymptotic solution for case (ii),  $\alpha_{>} < r_0a(r_0) < 0$  for  $r \rightarrow 0, \infty$  and  $C_1 \rightarrow 0, \infty$ .

		$r \rightarrow 0$	$r \rightarrow \infty$
A	$C_1 \rightarrow 0$	$r^{-1}$	$e^{\frac{1}{r}}$
	$C_1 \rightarrow \infty$	$r^{-\frac{1}{C_1}}$	$e^{\frac{1}{r}}$
Z	$C_1 \rightarrow 0$	$r^{-C_1}$	$e^{\frac{C_1}{r}}$
	$C_1 \rightarrow \infty$	$r^{-1}$	$e^{\frac{C_1}{r}}$
B	$C_1 \rightarrow 0$	$-C_1 - C_1^2$	$1 - \frac{1}{r} - \frac{C_1}{r} + \frac{C_1}{4r^2}$
	$C_1 \rightarrow \infty$	$-\frac{3}{4C_1}$	$1 - \frac{1}{r} - \frac{C_1}{r} + \frac{C_1}{4r^2}$

Note that for  $r \rightarrow \infty$  and  $C_1 \rightarrow 0$ ,  $e^{\frac{1}{r}} \sim 1 + \frac{1}{r} + \frac{1}{2r^2} + \dots$ , which tends to  $1 + \frac{1}{r}$ , has the same asymptotic behavior as in 4D. However, this specific behavior highlights that the second time dimension, even in the limit of  $C_1 \rightarrow 0$ , generates a solution that includes the four-dimensional solution, but adds supplementary terms.

(iii)  $r_0a(r_0) < \alpha_{<} < \alpha_{>} < 0$ : In this case,  $(ra)' < 0$ .

For  $r \rightarrow 0$ ,  $a$  behaves similarly to case (i) and (ii), with  $a \sim \frac{\alpha_{>}}{r}$ . As  $r \rightarrow \infty$ ,  $a$  behaves as  $a \sim -\frac{1}{r^2}$ . We perform a similar analysis as for cases (i, ii) and provide a summary of the asymptotic behavior for  $C_1 \rightarrow 0$  and  $C_1 \rightarrow \infty$  in Table 4.

**Table 4.** Asymptotic solution for case (iii),  $r_0a(r_0) < \alpha_< < \alpha_> < 0$  for  $r \rightarrow 0, \infty$  and  $C_1 \rightarrow 0, \infty$ .

		$r \rightarrow 0$	$r \rightarrow \infty$
A	$C_1 \rightarrow 0$	$r^{-1}$	$e^{\frac{1}{r}}$
	$C_1 \rightarrow \infty$	$r^{-\frac{1}{C_1}}$	$e^{\frac{1}{r}}$
Z	$C_1 \rightarrow 0$	$r^{-C_1}$	$e^{\frac{C_1}{r}}$
	$C_1 \rightarrow \infty$	$r^{-1}$	$e^{\frac{C_1}{r}}$
B	$C_1 \rightarrow 0$	$-C_1 - C_1^2$	$1 - \frac{1}{r} - \frac{C_1}{r} + \frac{C_1}{4r^2}$
	$C_1 \rightarrow \infty$	$-\frac{3}{4C_1}$	$1 - \frac{1}{r} - \frac{C_1}{r} + \frac{C_1}{4r^2}$

(iv)  $r_0a(r_0) > 0$ : In this last case,  $ra > 0$  and  $(ra)' < 0$  for all  $r > 0$ . With  $\alpha_{>} < 0$ , Equation (51) can be written as

$$\alpha_< \ln\left(1 - \frac{\alpha_>}{ra}\right) - \alpha_> \ln\left(1 - \frac{\alpha_<}{ra}\right) = \ln\left(\frac{r_{S,5D}}{r}\right). \tag{85}$$

In the limit  $r \rightarrow \infty$ ,  $a$  behaves like  $a \sim \frac{1}{r^2}$ , which is remarkably similar to cases (ii, iii). Now, let us explore a solution close to  $r_{S,5D}$  for slightly larger  $r$ . In this case, we can Taylor expand both sides of (85) and obtain

$$a \sim \frac{\frac{2}{\sqrt{C_1}}}{r\sqrt{\frac{r}{r_{S,5D}} - 1}} \tag{86}$$

$$z \sim \frac{2\sqrt{C_1}}{r\sqrt{\frac{r}{r_{S,5D}} - 1}}. \tag{87}$$

Thus, we have

$$A(r) \sim e^{\frac{4\arctan(\sqrt{\frac{r}{r_{S,5D}} - 1})}{\sqrt{C_1}}} \tag{88}$$

$$Z(r) \sim e^{4\sqrt{C_1}\arctan(\sqrt{\frac{r}{r_{S,5D}} - 1})} \tag{89}$$

$$B(r) \sim 1 + \frac{\frac{2}{\sqrt{C_1}}}{\sqrt{\frac{r}{r_{S,5D}} - 1}} + \frac{2\sqrt{C_1}}{\sqrt{\frac{r}{r_{S,5D}} - 1}} + \frac{1}{\frac{r}{r_{S,5D}} - 1}. \tag{90}$$

Note that in (90),  $1 + \frac{1}{\frac{r}{r_{S,5D}} - 1} = \left(1 - \frac{r_{S,5D}}{r}\right)^{-1} = B_{4D}$  when identifying the Schwarzschild radius  $r_S$  with  $r_{S,5D}$ . Therefore,  $B(r) \sim B_{4D}(r)$  as  $C_1 \rightarrow 0$ . Additionally,  $\left(1 - \frac{r_{S,5D}}{r}\right)^{-1}$  dominates over  $\frac{1}{\sqrt{\frac{r}{r_{S,5D}} - 1}}$  for all  $r > r_{S,5D}$ . Thus, the singularity of  $B$  at  $r = r_{S,5D}$  is of the form  $\left(1 - \frac{r_{S,5D}}{r}\right)^{-1}$ . However, as seen for the 4D solution, this singularity is purely mathematical and can be eliminated through coordinate transformations [30]. In that sense, the solutions for  $A$ ,  $Z$ , and  $B$  can be extended beyond the Schwarzschild radius towards the interior of the event horizon,  $r < r_{S,5D}$ .

For the two cases  $r \gtrsim r_{S,5D}$  and  $r \rightarrow \infty$ , Table 5 summarizes their behavior for  $C_1 \rightarrow 0$  and  $C_1 \rightarrow \infty$ . It is worth noting, once again, that for  $C_1 \rightarrow 0$ , the behavior of  $A$  and  $B$  resembles that of  $A_{4D}$  and  $B_{4D}$ .

**Table 5.** Asymptotic solution for case (iv),  $r_0a(r_0) > 0$  for  $r \gtrsim r_{S,5D}, \infty$ , and  $C_1 \rightarrow 0, \infty$ .

		$r \gtrsim r_{S,5D}$	$r \rightarrow \infty$
A	$C_1 \rightarrow 0$	$\frac{4\left(\frac{r}{r_{S,5D}} - 1\right)}{\sqrt{C_1}}$	$e^{-\frac{1}{r}}$
	$C_1 \rightarrow \infty$	1	$e^{-\frac{1}{r}}$
Z	$C_1 \rightarrow 0$	1	$e^{-\frac{C_1}{r}}$
	$C_1 \rightarrow \infty$	$4\sqrt{C_1} \left(\frac{r}{r_{S,5D}} - 1\right)$	$e^{-\frac{C_1}{r}}$
B	$C_1 \rightarrow 0$	$\left(1 - \frac{r_{S,5D}}{r}\right)^{-1}$	$1 + \frac{1}{r} + \frac{C_1}{r} + \frac{C_1}{4r^2}$
	$C_1 \rightarrow \infty$	$\frac{2\sqrt{C_1}}{\sqrt{\frac{r}{r_{S,5D}} - 1}}$	$1 + \frac{1}{r} + \frac{C_1}{r} + \frac{C_1}{4r^2}$

3.3. Approximate Solution Close to  $r = 0$

In this section, Equation (51) provides an implicit solution for  $a$ , which cannot be solved explicitly. However, since our focus is on understanding the physics near the central singularity, we can derive an approximate solution for  $a$  and, consequently, for the entire metric around  $r = 0$  using the implicit function theorem.

As seen in the previous section, all solution classes for  $r_0a(r_0) < 0$  (i–iii) exhibit similar behavior as  $r$  approaches zero, with the asymptotic behavior  $ra \sim \alpha_>$ . To derive an approximation for  $a$  around  $\alpha_>$ , we make the ansatz

$$ra = \alpha_> - r^\alpha g(r) \tag{91}$$

where  $\alpha = 1 - \frac{\alpha_>}{\alpha_<} \in (0, 1)$ . Inserting Equation (91) into (53) yields

$$\ln(r_{S,5D}) = \ln(-\alpha_> + r^\alpha g(r)) + \frac{\alpha_<}{\alpha_> - \alpha_<} \ln(g(r)) - \frac{\alpha_>}{\alpha_> - \alpha_<} \ln(\alpha_> - \alpha_< - r^\alpha g(r)). \tag{92}$$

Defining

$$F(u, v) = -\ln(r_{S,5D}) + \ln(-\alpha_> + uv) + \frac{\alpha_<}{\alpha_> - \alpha_<} \ln(v) - \frac{\alpha_>}{\alpha_> - \alpha_<} \ln(\alpha_> - \alpha_< - uv), \tag{93}$$

when  $v > 0$  and  $u$  are restricted to a small interval around 0, we observe that there exists a unique  $v_0$ , such that

$$F(0, v_0) = -\ln(r_{S,5D}) + \ln(-\alpha_>) + \frac{\alpha_<}{\alpha_> - \alpha_<} \ln(v_0) - \frac{\alpha_>}{\alpha_> - \alpha_<} \ln(\alpha_> - \alpha_<) = 0. \tag{94}$$

Additionally,  $\frac{\partial F}{\partial v(0, v_0)} \neq 0$ . Therefore, according to the implicit function theorem, there exists an approximate solution  $v(u) = v_0 + \dots$  such that  $F(u, v) = 0$  for small  $u$ . Translating  $u$  with  $r^\alpha$  and  $v = v_0 + \dots$  with  $g(r)$ , we find that (91) can be written as  $ra = \alpha_> - r^\alpha v_0 + \dots$ . Solving Equation (94) for  $v_0$  and inserting into (91) leads to the approximate solution

$$a \approx -\frac{2(1+C_1-\sqrt{1+C_1+C_1^2})}{C_1 r} - 2^{\frac{2(1+C_1)}{1+C_1+\sqrt{1+C_1+C_1^2}}} \left(\frac{C_1 r}{\sqrt{1+C_1+C_1^2}}\right)^{\frac{-1+C_1+\sqrt{1+C_1+C_1^2}}{1+C_1+\sqrt{1+C_1+C_1^2}}} \left(\left(1+C_1+\sqrt{1+C_1+C_1^2}\right)r_{S,5D}\right)^{\frac{2\sqrt{1+C_1+C_1^2}}{1+C_1+\sqrt{1+C_1+C_1^2}}} \tag{95}$$

around  $r = 0$ .

By performing similar calculations as in Section 3.2, we derive the set of solutions  $A = A(r)$ ,  $Z = Z(r)$ , and  $B = B(r)$ :

$$A(r) \approx K_1 r^{-\frac{2(1+C_1-\sqrt{1+C_1+C_1^2})}{C_1}} e^{\frac{2\sqrt{1+C_1+C_1^2}}{1+C_1+\sqrt{1+C_1+C_1^2}} \left(\frac{C_1 r}{\sqrt{1+C_1+C_1^2}}\right)^{\frac{2\sqrt{1+C_1+C_1^2}}{1+C_1+\sqrt{1+C_1+C_1^2}}} \frac{1}{(1+C_1+\sqrt{1+C_1+C_1^2})r_{S,5D}} \frac{1}{C_1 r_{S,5D}} \frac{1}{1+C_1+\sqrt{1+C_1+C_1^2}}}, \tag{96}$$

$$Z(r) \approx K_2 r^{-2(1+C_1-\sqrt{1+C_1+C_1^2})} e^{\frac{2\sqrt{1+C_1+C_1^2}}{1+C_1+\sqrt{1+C_1+C_1^2}} \left(\frac{C_1 r}{\sqrt{1+C_1+C_1^2}}\right)^{\frac{2\sqrt{1+C_1+C_1^2}}{1+C_1+\sqrt{1+C_1+C_1^2}}} \frac{1}{(1+C_1+\sqrt{1+C_1+C_1^2})r_{S,5D}} \frac{1}{C_1 r_{S,5D}} \frac{1}{1+C_1+\sqrt{1+C_1+C_1^2}}}, \tag{97}$$

$$B(r) \approx 2^{-2+\frac{2(1+C_1)}{1+C_1+\sqrt{1+C_1+C_1^2}}} C_1 r^2 \left(\frac{C_1 r}{\sqrt{1+C_1+C_1^2}}\right)^{-\frac{2(1+C_1)}{1+C_1+\sqrt{1+C_1+C_1^2}}} \left(\left(1+C_1+\sqrt{1+C_1+C_1^2}\right)r_{S,5D}\right)^{\frac{-4\sqrt{1+C_1+C_1^2}}{1+C_1+\sqrt{1+C_1+C_1^2}}} \left(4^{\frac{1+C_1}{1+C_1+\sqrt{1+C_1+C_1^2}} \left(\frac{C_1 r}{\sqrt{1+C_1+C_1^2}}\right)^{\frac{2\sqrt{1+C_1+C_1^2}}{1+C_1+\sqrt{1+C_1+C_1^2}}} - 4 \left(\left(1+C_1+\sqrt{1+C_1+C_1^2}\right)r_{S,5D}\right)^{\frac{2\sqrt{1+C_1+C_1^2}}{1+C_1+\sqrt{1+C_1+C_1^2}}}\right), \tag{98}$$

such that the total spacetime line element reads

$$ds^2 = A(r)c^2 dt^2 + Z(r)\gamma^2 d\tau^2 - B(r)dr^2 - r^2(d\theta^2 + \sin^2\theta d\varphi^2). \tag{99}$$

$K_{1,2}$  are integration constants. As mentioned in Section 3.2,  $A \sim r^{-1}$  and  $B \rightarrow 0$  for  $r \rightarrow 0$  and  $C_1 \rightarrow 0$ , which is consistent with the solutions  $A_{4D}$  (46) and  $B_{4D}$  (47) for four-dimensional spacetime. Specifically, we have

$$\lim_{C_1 \rightarrow 0} A = K_1 \frac{e^{-\frac{r}{r_{S,5D}}}}{r} \approx K_1 \left(\frac{1}{r} - \frac{1}{r_{S,5D}}\right). \tag{100}$$

For this limit to match the behavior of  $A_{4D}$ , we identify  $K_1 = -r_{S,5D}$  and  $r_{S,5D} = r_S = \frac{2GM}{c^2}$ . Similarly, the limits of  $Z$  for  $C_1 \rightarrow 0$  and  $C_1 \rightarrow \infty$  are

$$\lim_{C_1 \rightarrow 0} Z = K_2 \tag{101}$$

$$\lim_{C_1 \rightarrow \infty} Z = K_2 \frac{e^{-\frac{r}{r_{S,5D}}}}{r}. \tag{102}$$

Since the 4D solution ( $C_1 \rightarrow 0$ ) does not include  $Z$ , we set  $K_2 \approx 0$  to be a small value. This choice also eases the singularity at  $r = 0$  for  $C_1 \rightarrow \infty$ . It is interesting to observe that even for small  $K_2$ ,  $A$  exhibits a distinct behavior from  $A_{4D}$ .

Note that the method of using the implicit function theorem can be applied to approximate solutions at any other point in spacetime. This implies that the approach presented here can be extended to investigate the behavior of the metric at various locations beyond the central singularity.

#### 4. Physical Interpretation

In the case of  $A_{4D}$ , it is well known that it diverges to infinity as  $r \rightarrow 0$ , resulting in a singularity in spacetime. Given Equations (96)–(98) for  $r \approx 0$ , let us explore how  $A$  and  $B$  behave close to  $r = 0$ . Figure 1 depicts the absolute values  $|A|$  and  $|B|$  for the black hole Sgr A\* for different values of  $C_1$ , comparing them with the four-dimensional solutions

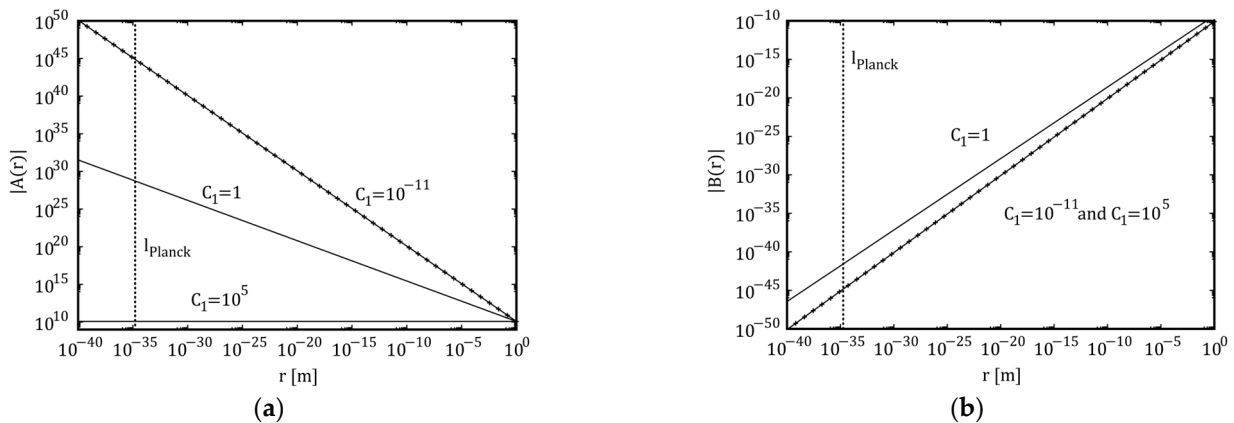
$|A_{4D}|$  (46) and  $|B_{4D}|$  (48). To accommodate a logarithmic scale and account for the fact that both  $A$  and  $B$  are negative for  $r < r_S$ , we plot the absolute values.

Figure 1 illustrates that  $A$  and  $B$  indeed tend to the four-dimensional solutions as  $C_1$  decreases towards zero. Moreover, it shows that  $B$  converges to zero when  $r \rightarrow 0$ , aligning with the behavior observed in the four-dimensional solution. However, for large values of  $C_1$ , the magnitude of  $A$  tends to  $r_S$  which is consistent with the limit

$$\lim_{C_1 \rightarrow \infty} |A(r)| = |K_1| = r_S < \infty. \tag{103}$$

Thus,  $A$  remains bounded and finite. This observation is in alignment with the asymptotic behavior for  $r \rightarrow 0$  and  $C_1 \rightarrow \infty$  discussed in Section 3.2 (see Tables 2–4). Also note that for such large values of  $C_1$ ,  $|A(r)| \approx r_S$  for small  $r \lesssim l_{Planck}$ , where  $l_{Planck} \approx 10^{-35}$  m denotes the Planck length. At scales below the Planck length, the laws of general relativity break down [31]. Previous calculations have indicated the potential influence of a second time dimension on small spatial scales in the order of the Planck length [23], including the vicinity of a black hole’s central mass. Subsequently, we cannot necessarily assume that  $C_1 \rightarrow 0$  within the event horizon. The existence of a second time dimension could potentially provide a viable solution to overcome the singularity at  $r = 0$ .

For large  $C_1$  around  $r = 0$ , the metric elements are regular, and so is the line element (99). Figure 2 shows the line element (99) and its four-dimensional equivalent  $ds_{4D}^2 = A_{4D}(r)c^2dt^2 - B_{4D}(r)dr^2 - r^2(d\theta^2 + \sin^2\theta d\varphi^2)$  with constants  $\theta$  and  $\varphi$  for the same situation depicted in Figure 1. While  $\theta = const.$  is justified by considering particle motion in the equatorial plane, we have chosen  $\varphi = const.$  to ease plotting. However, since there is no singularity in  $\varphi$ , this choice does not alter our conclusions. Figure 2 shows that the four-dimensional line element and the five-dimensional line element for small  $C_1$  diverge, as expected. On the contrary, for large  $C_1$  the 5D line element is regular beyond the Planck length. Hence, we conclude that the particle motion integrated over the infinitesimally small line element is non-singular as well.



**Figure 1.** The absolute values of the solutions (a)  $A(r)$  (96) and (b)  $B(r)$  (98) as a function of distance  $r$  from the central point at  $r = 0$  for Sgr A\* ( $r_S \approx 1.227 \cdot 10^{10}$  m [32]) for different  $C_1$ . The crosses indicate the four-dimensional solutions  $|A_{4D}(r)|$  and  $|B_{4D}(r)|$  (46, 47). The dotted line indicates the Planck length  $l_{Planck}$ .

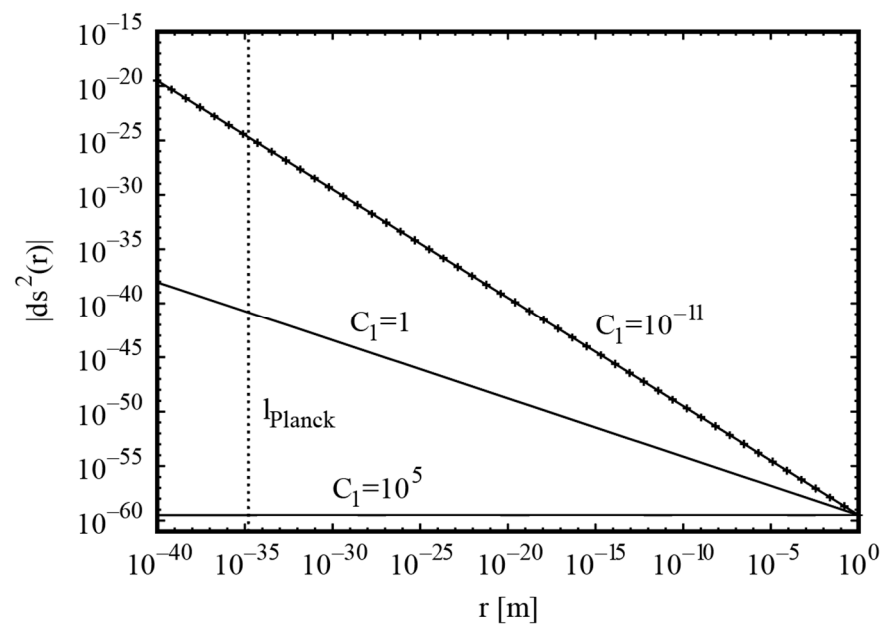


**Figure 2.** The five-dimensional line element (99) for the same situation as in Figure 1. The crosses indicate the four-dimensional line element  $ds_{4D}^2 = A_{4D}(r)c^2 dt^2 - B_{4D}(r)dr^2 - r^2(d\theta^2 + \sin^2\theta d\phi^2)$ . As numerical values, we have chosen  $\gamma = c$  [25],  $dr = l_{\text{Planck}}$ ,  $dt = d\tau = t_{\text{Planck}}$ , the Planck time, and  $K_2 = 10^{-40}$ .

## 5. Conclusions and Outlook

We have investigated the properties of non-rotating, non-charged Schwarzschild black holes within an extended spacetime incorporating two temporal dimensions with the aim of understanding the physics at the central singularity. We extended Einstein's field equations by one more time dimension and derived the corresponding equations for the 5D Schwarzschild metric. We have shown the existence of a solution which can also be applied to the 4D Schwarzschild metric. We explored various solution classes both inside and outside of the black hole's event horizon, and presented an approximate solution for the Schwarzschild metric in the proximity of the central singularity that remains consistent with the 4D solution. Notably, our proposed solution effectively overcomes the singularity quandary associated with black holes, providing valuable insights into their fundamental properties within this augmented framework. As we currently cannot investigate the interior of black holes, we cannot exclude the potential influence of additional dimensions effectively acting on small spatial scales in the order of the Planck length [25]. Thus, we have seen that in the vicinity of the central black hole mass, a second time dimension keeps the metric bounded rather than diverging to infinity. Thus, we have found a solution to the singularity problem of black holes. This work serves as a steppingstone for further investigations into black holes, alternative spacetime metrics, additional dimensions, and the underlying mathematical implications, ultimately providing a deeper understanding of the nature and significance of black holes in the Universe.

In the future, we are planning to extend our work to more dimensions and metrics and make predictions of observational effects of additional time dimensions. This includes the solution of Einstein's field equations for the Kerr metric describing rotating black holes, which will be based on the current work on Schwarzschild black holes. Additionally, we plan to develop a numerical framework to solve the geodesic equations in the vicinity of the central mass. By doing so, we will be able to investigate particle orbits around the event horizon in extended spacetime which will let us predict the particle motion around black holes. This will finally allow us to make observational predictions of the physics around the event horizon and ergosphere of rotating black holes, which can be compared with future observations.

**Author Contributions:** Conceptualization, M.P., H.C. and C.K.; Formal analysis, M.P., H.C. and C.K.; Investigation, M.P., H.C. and C.K.; Methodology, M.P., H.C. and C.K.; Supervision, H.C. and C.K.; Writing—original draft, M.P., H.C. and C.K. All authors have read and agreed to the published version of the manuscript.

**Funding:** This research received no external funding.

**Institutional Review Board Statement:** Not applicable.

**Data Availability Statement:** The data are contained within the article.

**Conflicts of Interest:** The authors declare no conflict of interest.

## References

1. Brüggmann, B.; Ghez, A.M.; Greiner, J. Black holes. *Proc. Natl. Acad. Sci. USA* **2001**, *98*, 10525–10526. [[CrossRef](#)] [[PubMed](#)]
2. Misner, C.W.; Thorne, K.S.; Wheeler, J.A. *Gravitation*; W. H. Freeman and Company: San Francisco, CA, USA, 1970.
3. Einstein, A. *Relativity: The Special and General Theory*; Henry Holt and Company: New York, NY, USA, 1920.
4. Schwarzschild, K. On the Gravitational Field of a Mass Point According to Einstein's Theory. *Sitzungsber. Kgl. Preuß. Akad. Wiss.* **1916**, *7*, 189–196.
5. Kerr, R.P. Gravitational Field of a Spinning Mass as an Example of Algebraically Special Metrics. *Phys. Rev. Lett.* **1963**, *11*, 237. [[CrossRef](#)]
6. Newman, E.T.; Couch, E.; Chinnapared, K.; Exton, A.; Prakash, A.; Torrence, R. Metric of a Rotating, Charged Mass. *J. Math. Phys.* **1965**, *6*, 918. [[CrossRef](#)]
7. Reissner, H. Über die Eigengravitation des elektrischen Feldes nach der Einsteinschen Theorie. *Ann. Phys.* **1916**, *355*, 106–120. [[CrossRef](#)]
8. Weyl, H. Zur Gravitationstheorie. *Ann. Phys.* **1917**, *359*, 117–145. [[CrossRef](#)]
9. Nordström, G. On the Energy of the Gravitation field in Einstein's Theory. *K. Ned. Akad. Wet. Proc.* **1918**, *20*, 1238–1245.
10. Jeffery, G.B. The field of an electron on Einstein's theory of gravitation. *Proc. R. Soc. A* **1921**, *99*, 123.
11. Penrose, R. Gravitational Collapse and Space-Time Singularities. *Phys. Rev. Lett.* **1965**, *14*, 57. [[CrossRef](#)]
12. Akiyama, K.; Alberdi, A.; Alef, W.; Asada, K.; Azulay, R.; Baczkowski, A.-K.; Ball, D.; Baloković, M.; Barrett, J.; Bintley, D.; et al. First M87 Event Horizon Telescope Results. I. The Shadow of the Supermassive Black Hole. *Astrophys. J. Lett.* **2019**, *875*, 17.
13. Alberdi, A.; Alef, W.; Algaba, J.C.; Anantua, R.; Asada, K.; Azulay, R.; Bach, U.; Baczkowski, A.-K.; Ball, D.; Baloković, M.; et al. First Sagittarius A\* Event Horizon Telescope Results. I. The Shadow of the Supermassive Black Hole in the Center of the Milky Way. *Astrophys. J. Lett.* **2022**, *930*, 21.
14. Gambini, R.; Pullin, J. Black Holes in Loop Quantum Gravity: The Complete Space-Time. *Phys. Rev. Lett.* **2008**, *101*, 1301. [[CrossRef](#)] [[PubMed](#)]
15. Pullin, J.; Gambini, R. *A First Course in Loop Quantum Gravity*; Oxford University Press: Oxford, UK, 2011.
16. Zwiebach, B. *A First Course in String Theory*; Cambridge University Press: Cambridge, UK, 2004.
17. Vaz, C. Black holes as gravitational atoms. *J. Mod. Phys.* **2014**, *D23*, 1441002. [[CrossRef](#)]
18. Corda, C. Black Hole Spectra from Vaz's Quantum Gravitational Collapse. *Fortschr. Phys.* **2023**, *71*, 2300028. [[CrossRef](#)]
19. Bars, I. Supersymmetry, p-brane duality, and hidden spacetime dimensions. *Phys. Rev. D* **1996**, *54*, 5203. [[CrossRef](#)]
20. Bars, I.; Kounnas, C. Theories with Two Times. *Phys. Lett. B* **1997**, *402*, 25–32. [[CrossRef](#)]
21. Bars, I.; Kounnas, C. String and particle with two times. *Phys. Rev. D* **1997**, *56*, 3664. [[CrossRef](#)]
22. Tegmark, M. On the dimensionality of spacetime. *Class. Quantum Gravity* **1997**, *14*, L69. [[CrossRef](#)]
23. Köhn, C. The Planck Length and the Constancy of the Speed of Light in Five Dimensional Spacetime Parametrized with Two Time Coordinates. *J. High Energy Phys. Gravit. Cosmol.* **2017**, *3*, 635–650. [[CrossRef](#)]
24. Chen, X. Three Dimensional Time Theory: To Unify the Principles of Basic Quantum Physics and Relativity. *arXiv* **2005**, arXiv:quant-ph/0510010.
25. Köhn, C. A Solution to the Cosmological Constant Problem in Two Time Dimensions. *J. High Energy Phys. Gravit. Cosmol.* **2020**, *6*, 640–655. [[CrossRef](#)]
26. Elsborg, J.; Köhn, C. Magnetic monopoles in two time dimensions. *Int. J. Mod. Phys. A* **2022**, *37*, 2250141. [[CrossRef](#)]
27. Weinstein, S. Multiple Time Dimensions. *arXiv* **2008**, arXiv:0812.3869.
28. Craig, W.; Weinstein, S. On determinism and well-posedness in multiple time dimensions. *Proc. R. Soc. A* **2009**, *465*, 3023–3046. [[CrossRef](#)]
29. Lindelöf, E. Sur l'application de la méthode des approximations successives aux équations différentielles ordinaires du premier ordre. *C. R. Hebd. Séances Acad. Sci.* **1894**, *118*, 454–457.
30. Landau, L.D.; Lifshitz, E.M. *The Classical Theory of Fields*, 3rd ed.; Pergamon Press: London, UK, 1971; Volume 2.

31. Debono, I.; Smoot, G.F. General Relativity and Cosmology: Unsolved Questions and Future Directions. *Universe* **2016**, *2*, 23. [[CrossRef](#)]
32. Lo, K.Y.; Shen, Z.-Q.; Zhao, J.-H.; Ho, P.T.P. Intrinsic Size of Sagittarius A\*: 72 Schwarzschild Radii. *Astrophys. J.* **1998**, *508*, L61. [[CrossRef](#)]

**Disclaimer/Publisher's Note:** The statements, opinions and data contained in all publications are solely those of the individual author(s) and contributor(s) and not of MDPI and/or the editor(s). MDPI and/or the editor(s) disclaim responsibility for any injury to people or property resulting from any ideas, methods, instructions or products referred to in the content.